Electronic Supplementary Material (ESI) for Journal of Materials Chemistry A.

A biomimetic Setaria viridis-inspired electrode with polyaniline nanowire arrays aligned on MoO3@polypyrrole core-shell nanobelts

Ying Liu,[a] Le Li,[a] Jixin Zhu,[b] Jingsan Xu,[c] Siliang Liu,[a] Yufeng Wang,[a] Chao Zhang*[a] and Tianxi Liu*[a]

[a] State Key Laboratory for Modification of Chemical Fibers and Polymer Materials, College of Materials Science and Engineering, Innovation Center for Textile Science and Technology, Donghua University, Shanghai 201620, P. R. China

[b] Shaanxi Institute of Flexible Electronics (SIFE), Northwestern Polytechnical University (NPU), 127 West Youyi Road, Xi'an 710072, China

[c] School of Chemistry, Physics and Mechanical Engineering, Queensland University of Technology, Brisbane, QLD 4001, Australia

* E-mail: czhang@dhu.edu.cn (C. Zhang)

* E-mail: txliu@fudan.edu.cn or txliu@dhu.edu.cn (T. X. Liu)

Electronic Supplementary Information

Figure captions:

Fig. S1 SEM images of the MoO_3 powder after grinding at (a) low and (b) high magnifications, respectively.

Fig. S2 SEM images of (a) MoO_3/PPy-1 and (b) MoO_3/PPy-3.

Fig. S3 SEM images of neat PPy.

Fig. S4 SEM images of neat PANI.

Fig. S5 Schematic illustration of the formation of MoO_3/PANI/PPy composites.

Fig. S6 SEM images of (a) MoO_3/PANI-1, (b) MoO_3/PANI-2 and (c) MoO_3/PANI-3.

Fig. S7 TEM images of (a, b) MoO_3/PANI-2 and (c, d) MoO_3/PANI/PPy composites at low and high magnifications, respectively.

Fig. S8 SEM images of MoO_3/PANI/PPy composites at (a) low and (b) high magnifications, respectively.

Fig. S9 (a) Comparison of CV curves of MoO_3/PPy-1, MoO_3/PPy-2 and MoO_3/PPy-3 at a scan rate of 10 mV s^{-1}. (b) Specific capacitances of MoO_3/PPy-1, MoO_3/PPy-2 and MoO_3/PPy-3 at various current densities.

Fig. S10 (a) Comparison of CV curves of MoO_3/PANI-1, MoO_3/PANI-2 and MoO_3/PANI-3 at a scan rate of 10 mV s^{-1}. (b) Specific capacitances of MoO_3/PANI-1, MoO_3/PANI-2 and MoO_3/PANI-3 at various current densities.

Fig. S11 CV curves of MoO_3/PANI/PPy electrode at various scan rates of 5, 20, 50, 100 and 200 mV s^{-1}, respectively.

Fig. S12 TGA curves of MoO_3, MoO_3/PPy and MoO_3/PPy/PANI in air.

Fig. S13 Specific capacitances of MoO_3/PANI/PPy at various current densities.

Fig. S14 Self-discharge measurement of the supercapacitor based on the two-electrode MoO_3/PPy/PANI electrodes

Fig. S15 Galvanostatic charge/discharge curves of MoO_3, PANI, PPy, MoO_3/PANI, MoO_3/PPy, MoO_3/PPy/PANI electrodes for 3000 charge/discharge cycles at a current density of 2 A g^{-1}.

Fig. S16 (a) Cycling stability of the MoO_3/PPy/PANI electrode after 20000 charge/discharge cycles at 10 A g^{-1}. The corresponding galvanostatic charge/discharge curves of the MoO_3/PPy/PANI electrodes for (b) 101~110 and (c) 19991~20000 charge/discharge cycles at a current density of 10 A g^{-1}.

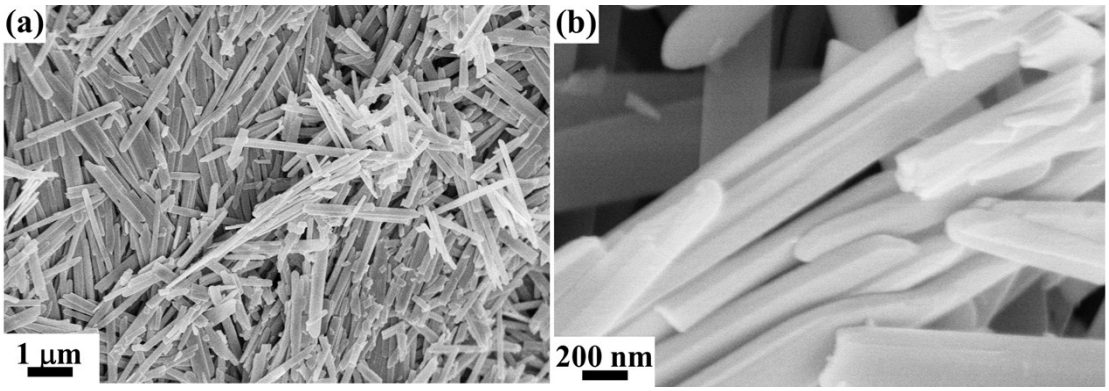

Fig. S1 SEM images of the MoO_3 powder after grinding at (a) low and (b) high magnifications, respectively.

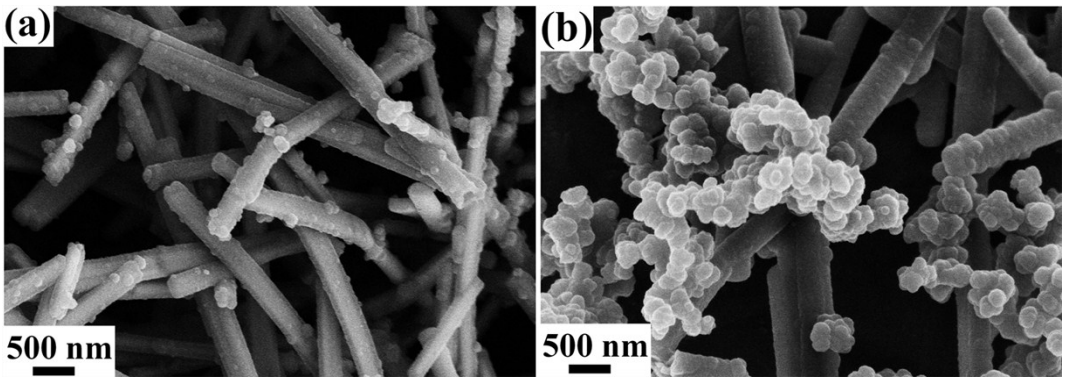

Fig. S2 SEM images of (a) MoO_3/PPy-1 and (b) MoO_3/PPy-3.

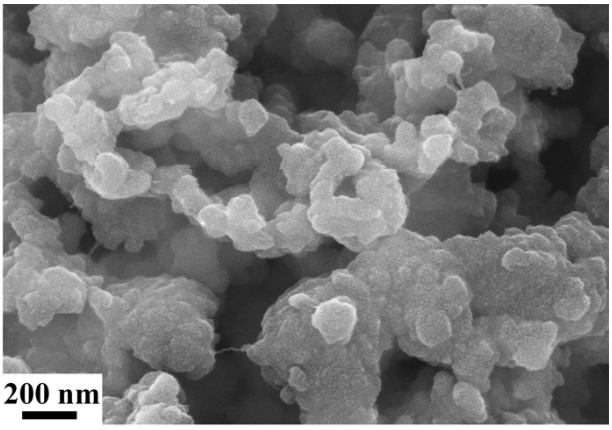

Fig. S3 SEM images of neat PPy.

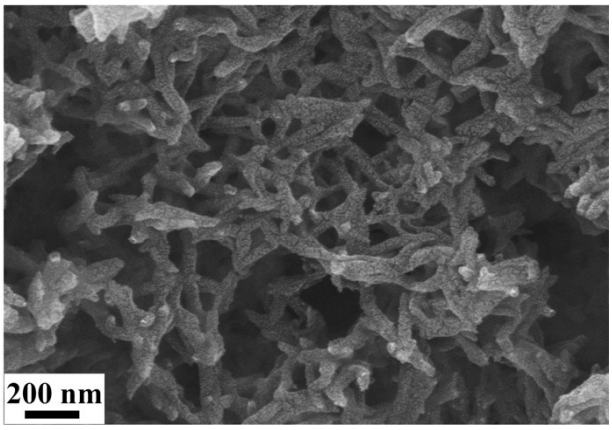

Fig. S4 SEM images of neat PANI.

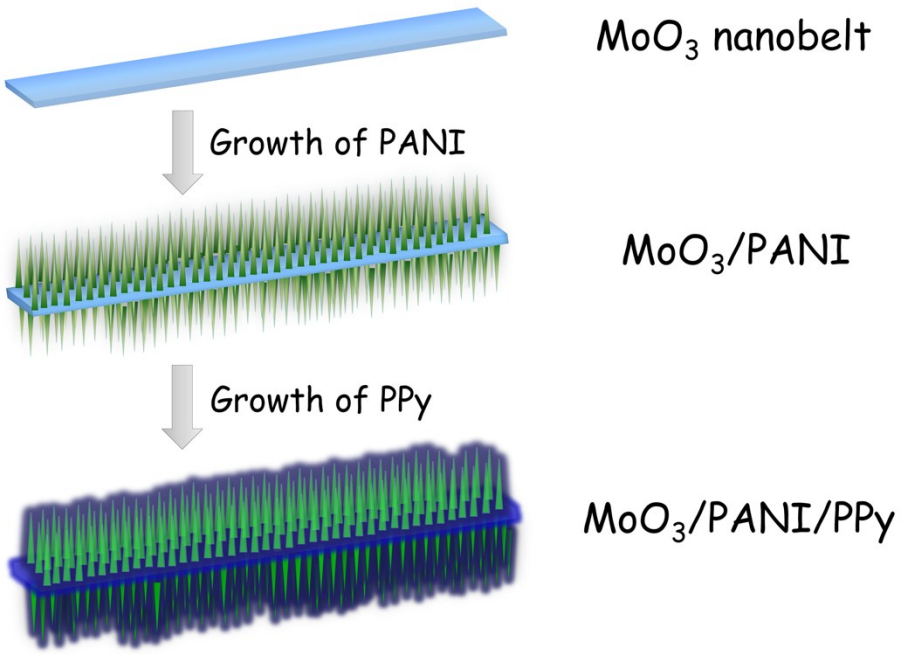

Fig. S5 Schematic illustration of the formation of MoO_3/PANI/PPy composites.

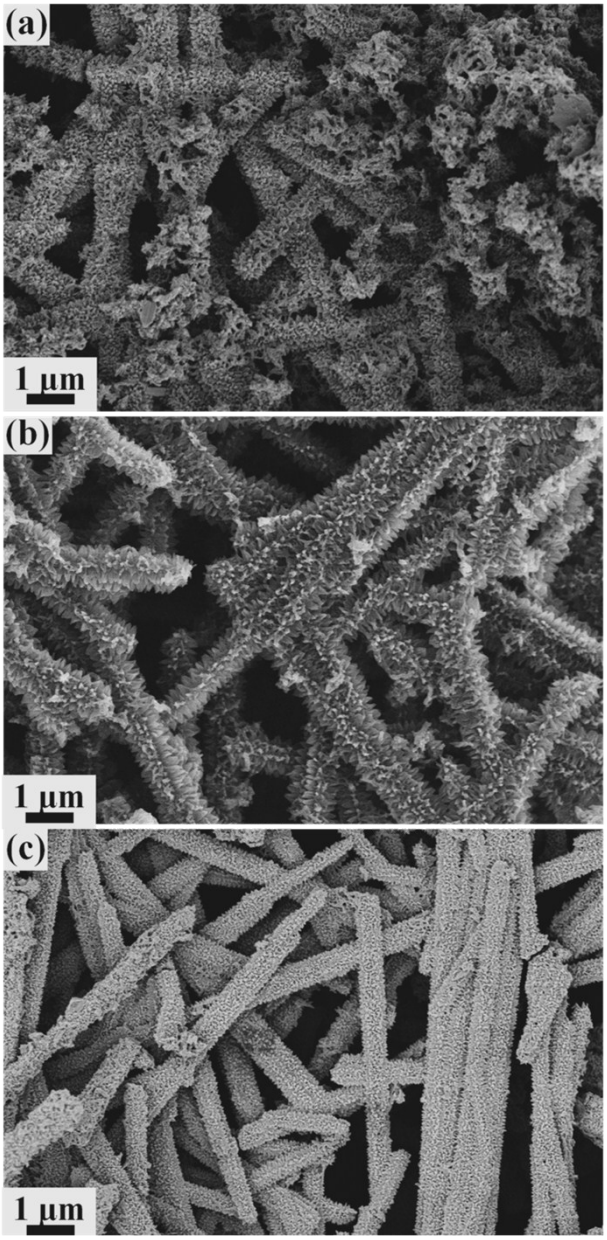

Fig. S6 SEM images of (a) MoO_3/PANI-1, (b) MoO_3/PANI-2 and (c) MoO_3/PANI-3.

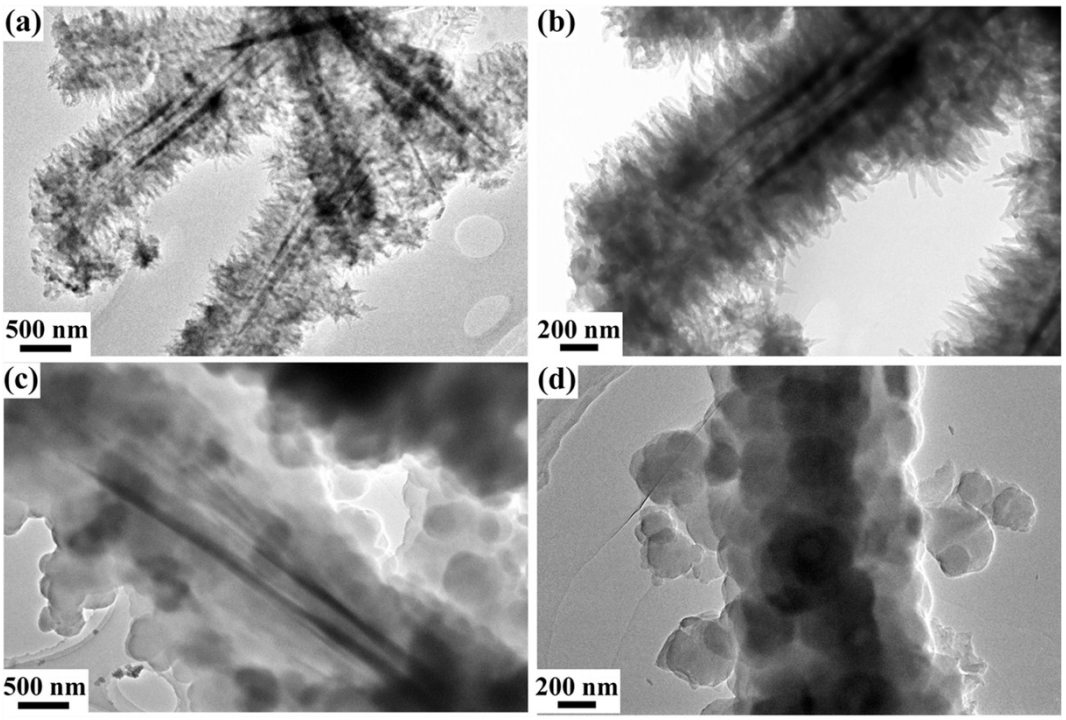

Fig. S7 TEM images of (a, b) MoO_3/PANI-2 and (c, d) MoO_3/PANI/PPy composites at low and high magnifications, respectively.

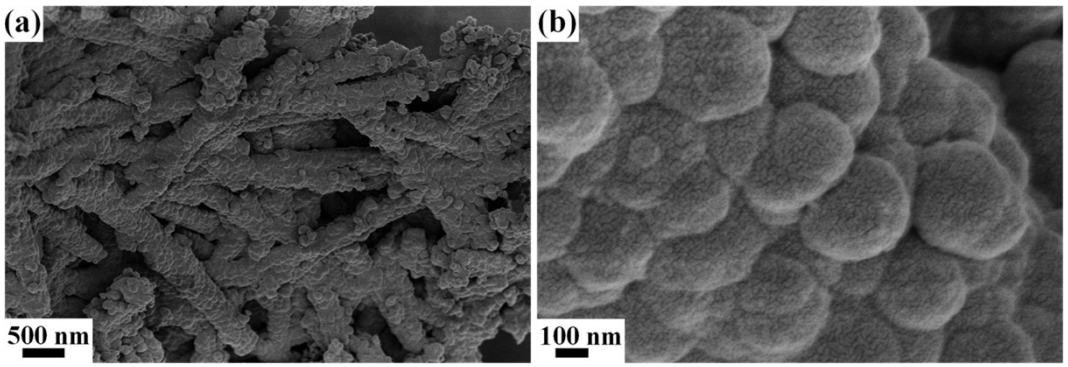

Fig. S8 SEM images of MoO_3/PANI/PPy composites at (a) low and (b) high magnifications, respectively.

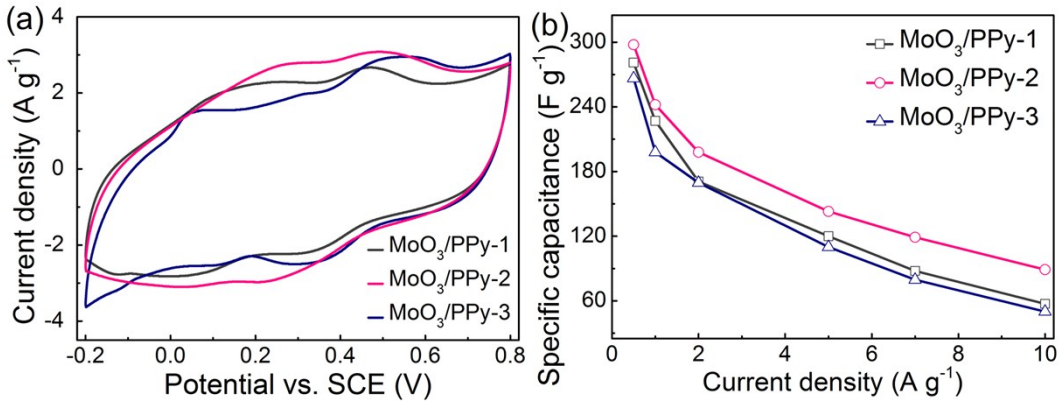

Fig. S9 (a) Comparison of CV curves of MoO_3/PPy-1, MoO_3/PPy-2 and MoO_3/PPy-3 at a scan rate of 10 mV s^{-1}. (b) Specific capacitances of MoO_3/PPy-1, MoO_3/PPy-2 and MoO_3/PPy-3 at various current densities.

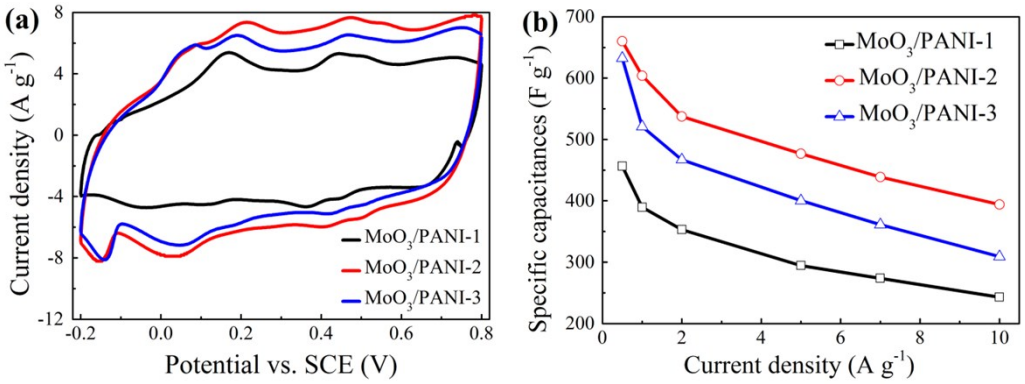

Fig. S10 (a) Comparison of CV curves of MoO_3/PANI-1, MoO_3/PANI-2 and MoO_3/PANI-3 at a scan rate of 10 mV s^{-1}. (b) Specific capacitances of MoO_3/PANI-1, MoO_3/PANI-2 and MoO_3/PANI-3 at various current densities.

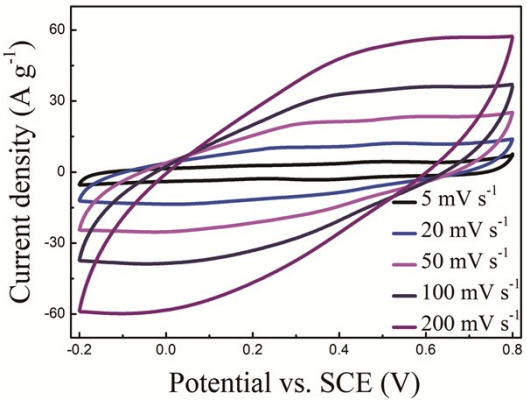

Fig. S11 CV curves of MoO_3/PANI/PPy electrode at various scan rates of 5, 20, 50, 100 and 200 mV s^{-1}, respectively.

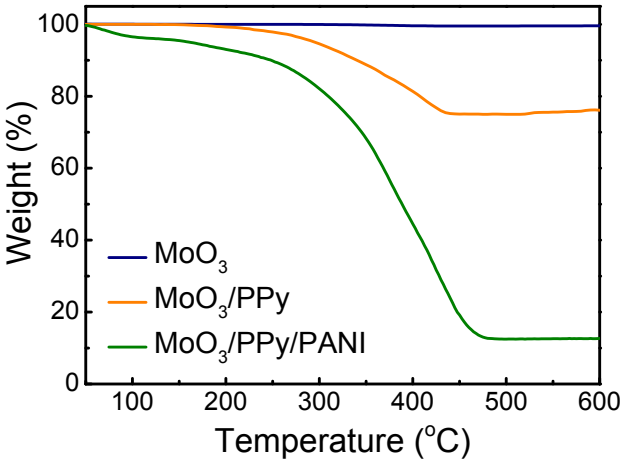

Fig. S12 TGA curves of MoO_3, MoO_3/PPy and MoO_3/PPy/PANI in air.

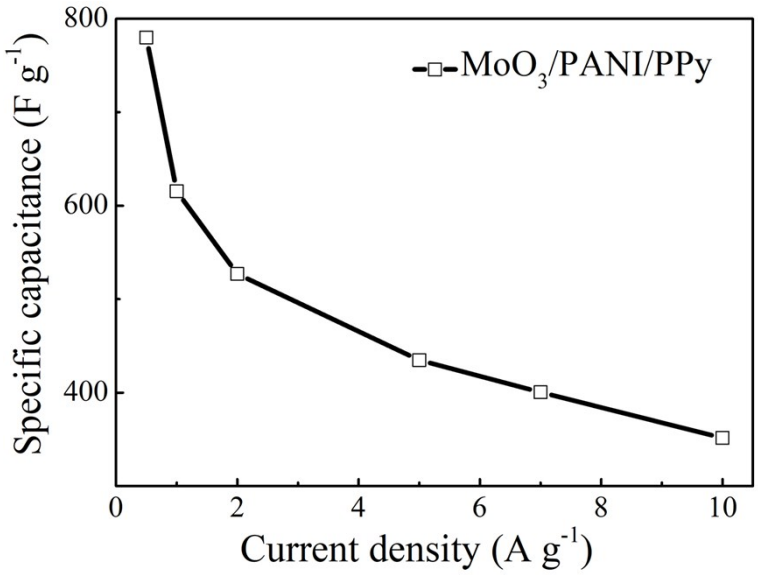

Fig. S13 Specific capacitances of MoO_3/PANI/PPy at various current densities.

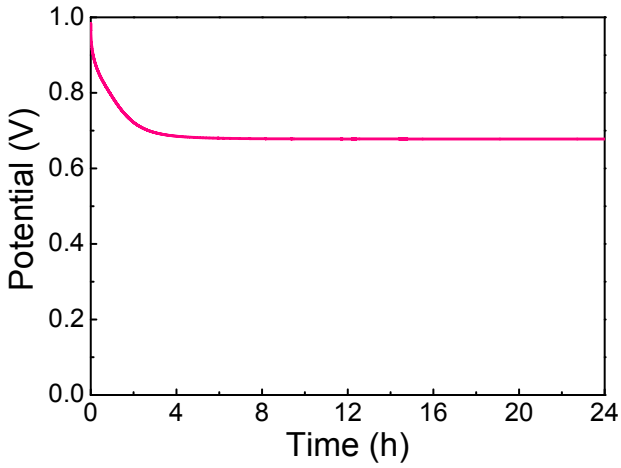

Fig. S14 Self-discharge measurement of the supercapacitor based on the two-electrode MoO_3/PPy/PANI electrodes

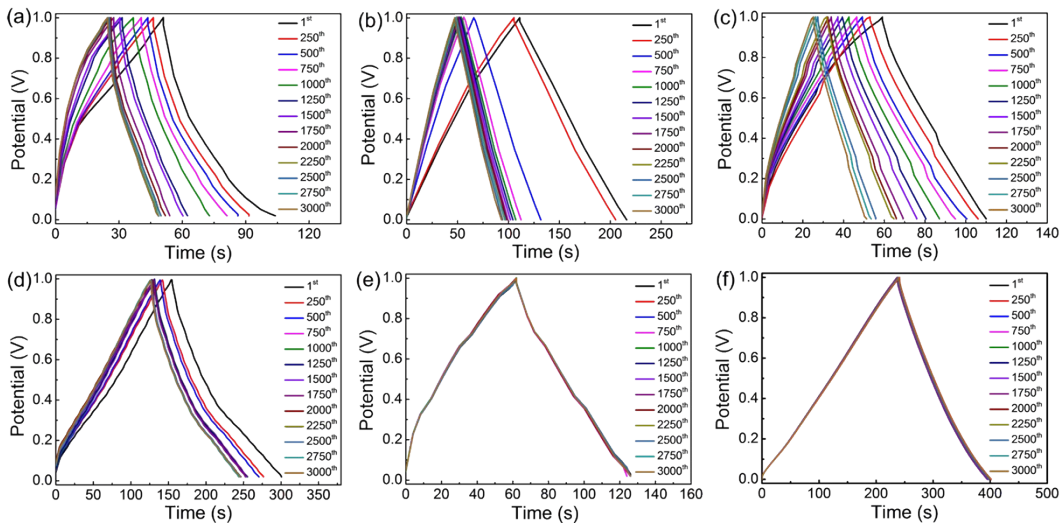

Fig. S15 Galvanostatic charge/discharge curves of MoO_3, PANI, PPy, MoO_3/PANI, MoO_3/PPy, MoO_3/PPy/PANI electrodes for 3000 charge/discharge cycles at a current density of 2 A g^{-1}.

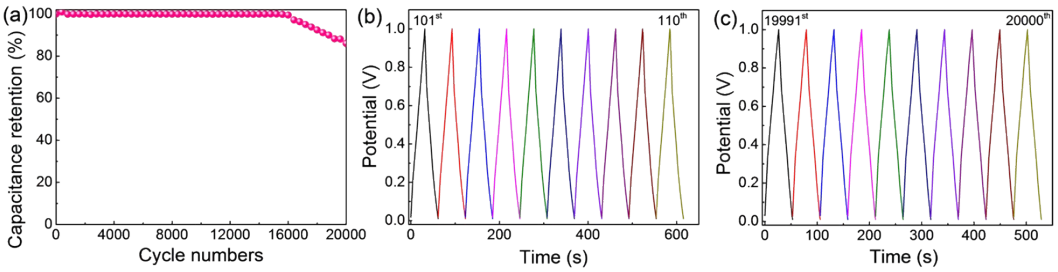

Fig. S16 (a) Cycling stability of the MoO_3/PPy/PANI electrode after 20000 charge/discharge cycles at 10 A g^{-1}. The corresponding galvanostatic charge/discharge curves of the MoO_3/PPy/PANI electrodes for (b) 101~110 and (c) 19991~20000 charge/discharge cycles at a current density of 10 A g^{-1}.